

MICROSTRUCTURE AND MAGNETIC PROPERTIES OF NdFeB SINTERED MAGNETS DIFFUSION-TREATED WITH Cu/Al MIXED DyCo ALLOY-POWDER

We investigated the microstructural and magnetic property changes of DyCo, Cu + DyCo, and Al + DyCo diffusion-treated NdFeB sintered magnets. The coercivity of all diffusion treated magnet was increased at 880°C of 1st post annealing(PA), by 6.1 kOe in Cu and 7.0 kOe in Al mixed DyCo coated magnets, whereas this increment was found to be relatively low (3.9 kOe) in the magnet coated with DyCo only. The diffusivity and diffusion depth of Dy were increased in those magnets which were treated with Cu or Al mixed DyCo, mainly due to comparatively easy diffusion path provided by Cu and Al because of their solubility with Nd-rich grain boundary phase. The formation of Cu/Al-rich grain boundary phase might have enhanced the diffusivity of Dy-atoms. Moreover, relatively a large number of Dy atoms reached into the magnet and mostly segregated at the interface of Nd₂Fe₁₄B and grain boundary phases covering Nd₂Fe₁₄B grains so that the core-shell type structures were developed. The formation of highly anisotropic (Nd, Dy)₂Fe₁₄B phase layer, which acted as the shell in the core-shell type structure so as to prevent the reverse domain movement, was the cause of enhancing the coercivity of diffusion treated NdFeB magnets. Segregation of cobalt in Nd-rich TJP followed by the formation of Co-rich phase was beneficial for the coercivity enhancement, resulting in the stabilization of the metastable c-Nd₂O₃ phase.

Keywords: Nd-Fe-B sintered magnet, grain boundary diffusion process, low melting-point elements, DyCo alloy-powder diffusion

1. Introduction

Grain boundary diffusion treatment has been proposed as a heavy rare-earth (HRE) elements saving method, where HRE atoms are allowed to diffuse via grain boundary [1,2]. However, the controlled diffusion phenomenon to achieve its optimum effect for the improvement of magnetic properties has still been a challenge. Developing the core-shell microstructure is known to be the most effective way to enhance the coercivity, and reduce the Dy content. The mechanism of magnetic reversal in the NdFeB sintered magnet is mainly due to the nucleation of reverse magnetic domains in the grain boundary area [3-5]. Therefore, targeting the Dy to the regions around the grain boundary could enhance coercivity, thereby minimizing the reduction in remanence. Many researchers have referred to this microstructure as the “core-shell microstructure” [6-13], which can be easily obtained by the grain boundary diffusion process (GBDP) [6-8] using HRE such as Dy. However, GBDP has a limitation of diffusion depth since NdFeB sintered body becomes fully dense during sintering process.

On the other hand, microstructural optimization by controlling diffusion behavior of HRE atoms with the aid of appropriate

material is of great interest. For this, Cu and Al could be effective promoters of diffusion of HRE atoms like Dy by improving wettability of Nd-rich grain boundary phase. The solubility limit of Cu with Nd₂Fe₁₄B phase is almost negligible, diffusion of Cu occurs only through grain boundaries whereas Al has the solubility to the Nd₂Fe₁₄B phase [3,4].

Cobalt in NdFeB sintered magnet is beneficial for the improvement of remanence and Curie temperature but the creation of planar anisotropy in main phase decreases the coercivity [9,10]. However, in real case, Co concentration is found to be higher in Nd-rich phase of NdFeB sintered magnets, which results in considerable microstructural change of Nd-rich phase. The low melting element like Cu increases the wettability and continuity of Nd-rich phase thereby increasing the coercivity [11].

In this work, we paid an effort to investigate the role of low melting point elements such as Cu and Al on Dy diffusion behavior and corresponding effect on magnetic and microstructural properties after being mixed with DyCo alloy-powder used for diffusion treatment. These elements could provide comparatively an easy path for Dy to diffuse via grain boundary into the interior of a magnet rather than in the case where only Dy-compounds were used for diffusion treatment. The coercivity of the diffu-

* DEPT. OF ADVANCED MATERIALS ENGINEERING, SUNMOON UNIVERSITY, ASAN, CHUNGNAM 336-708, KOREA

** DEPT. OF MATERIALS SCIENCE AND ENGINEERING, KOREA UNIVERSITY, SEOUL 136-713, KOREA

*** R&D CENTER OF JAHWA ELECTRONICS CO. LTD, CHEONGWON 363-922, KOREA

Corresponding author: tsjang@sunmoon.ac.kr

sion processed magnets which were treated with Cu or Al mixed Dy-source was improved by increasing diffusivity of Dy without much deterioration of remanence and energy product.

2. Experimental

Magnetic powder having average particle size of 3 μm with the composition of $\text{Nd}_{29.00}\text{Dy}_{3.00}\text{Fe}_{\text{Bal.}}\text{B}_{0.97}\text{M}_{2.39}$ (wt.%, M = Cu, Al, Co and Nb) was taken in this study for the magnet preparation. Also, DyCo alloy-powder of average particle size 152 μm was chosen as the Dy-source. The magnet samples were prepared through the powder metallurgical route and sintered at 1060°C for 4 hours. The sintered bulk magnet samples were cut into pieces of dimension 12.5 mm \times 12.5 mm \times 5 mm and were polished to remove the oxidized surface layer. Further, the polished samples were dipped in the solution prepared from the powders of DyCo(1.0 g), Cu or Al(0.2 g), and absolute ethanol(1 g). Three kinds of solutions; DyCo, Cu + DyCo, and Al + DyCo were prepared as the Dy supplier for diffusion treatment. Ultrasonic vibration was provided to make uniform coating layer of the Dy-source on the magnet surface. In a while, those Dy-source coated samples were annealed in three stages; 1st stage annealing was performed at 880°C for 8 hours, and the 2nd and 3rd stage at 530°C and 500°C for 2 hours each in vacuum ($\sim 10^{-5}$ Torr). Magnetic properties of the magnet samples were measured using a B-H loop tracer (Magnet-Physik Permagraph C-300). Microstructural investigation was carried out using a scanning electron microscopy (SEM, JXA-8500F) and High Resolution Transmission Electron Microscopy (HRTEM, JEOL JEM 2100F).

3. Results and discussion

Fig. 1 shows a comparison of the coercivity with three kinds of Dy-sources; DyCo only, Cu + DyCo and Al + DyCo. The coercivity of all diffusion-treated magnets was increased

at 880°C of heat treatment, the coercivity of Cu dipped magnet increased by 6.1 kOe and that of Al dipped magnet increased by 7.0 kOe. The increment of coercivity was found to be relatively low (3.9 kOe) in the magnet coated with DyCo only. We observed that both Cu and Al had almost similar effect on coercivity improvement particularly in the heat treatment temperature. Our previous result showed that there was critical changes in the microstructure of Nd-rich triple junction phase (TJP) and grain boundary phase (GBP).

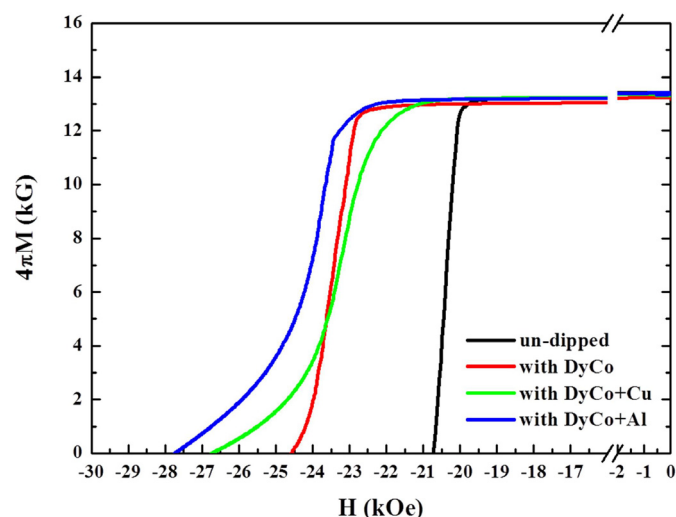


Fig. 1. Demagnetization curves of DyCo, Cu+DyCo and Al+DyCo dipped magnets

Fig. 2 shows the cross-sectional EPMA mapping images of (a) DyCo only, (b) DyCo+Cu, and (c) DyCo+Al dipped magnets with 1st PA at 880°C. As shown in Fig. 2b, Dy diffusion depth was increased as compared with the magnet treated with DyCo only (from 90 μm to 450 μm). A Nd-rich core-shell type structure was formed almost at the surface region. This indicates that Dy diffused into the main phase. The Cu was segregated at Nd-rich triple junction phase because Cu has poor solubility

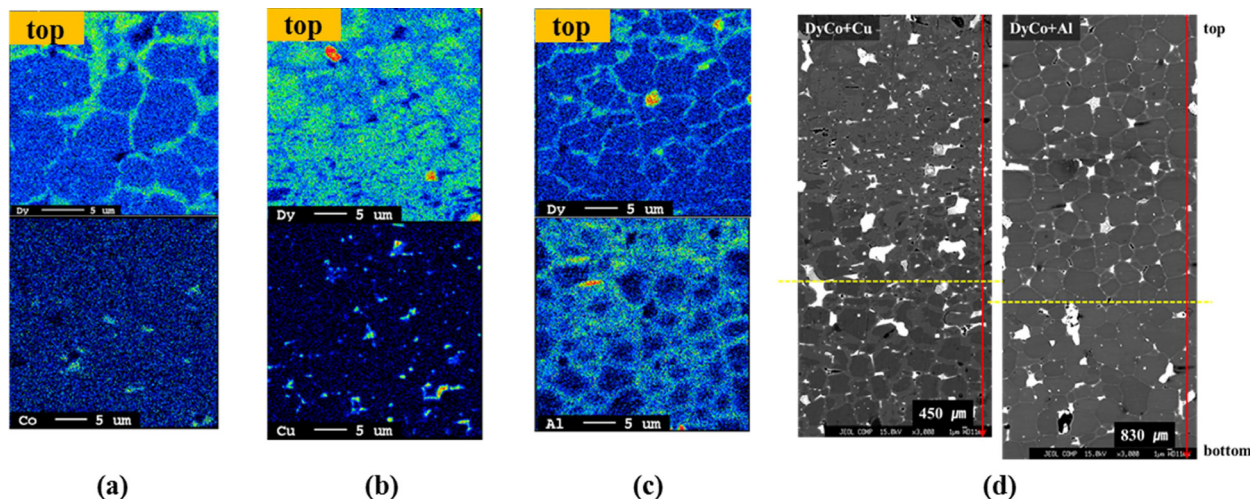


Fig. 2. Cross-sectional EPMA images of the surface area of (a) DyCo, (b) Cu + DyCo, and (c) Al + DyCo dipped magnets. The formation depth of core-shell type grains due to the Cu-driven and Al-driven Dy source is shown in (d)

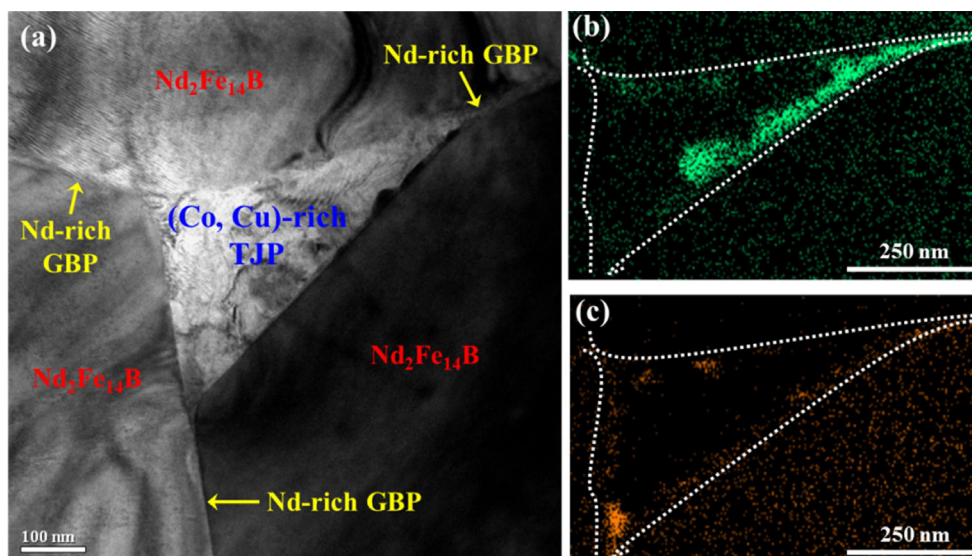


Fig. 3. (a) The bright field micrograph, (b) EDX mapping of Cu at Nd-rich TJP, and (c) EDX mapping of Co at Nd-rich TJP of the DyCo dipped magnet

with $\text{Nd}_2\text{Fe}_{14}\text{B}$ phase. In case of Al mixed DyCo treated magnet (Fig. 2c), it was observed that the Dy diffusion depth was considerably increased to $\sim 830 \mu\text{m}$. Al was distributed in grain boundary phases and outer area of the main phases as a result of the fact that Al was soluble in the main phase. The results from these observation indicate different diffusion behavior of Cu and Al on the NdFeB sintered magnet. Owing to the improvement in distribution of Dy, and increased diffusion depth of the Dy atoms, the coercivity was enhanced by increasing the fraction of Al added during the GBDP.

Fig. 3(a) shows the TEM bright field image of the two-step annealed one, and (b) and (c) shows the EDX images of Cu and Co distribution in (Co, Cu)-rich TJP, respectively. In general, Nd-rich TJP is composed of Nd-Co-Cu-O. The EDX mapping shown in Fig. 3 revealed that Cu and Co are not mixed perfectly throughout the TJP but separated to form Cu-rich and Co-rich region with approximate composition of $\text{Nd}_{32.5}\text{Co}_{2.6}\text{Cu}_{30.2}\text{O}_{34.8}$ and $\text{Nd}_{32.9}\text{Co}_{39.4}\text{Cu}_{12.7}\text{O}_{13.7}$ (in at. %), respectively. On the other hand, the Cu and Co poor region (dark contrast in TJP) has the composition of $\text{Nd}_{44.3}\text{Co}_{0.25}\text{Cu}_{0.43}\text{O}_{51.2}$. In case of Co and Nd, the eutectic decomposition reaction can occur at $\sim 630^\circ\text{C}$. Therefore, $\text{L} \leftrightarrow \text{Nd} + \text{Nd}_3\text{Co}$ eutectic reaction can occur during 1st PSA. Because of this eutectic decomposition, the TJP has Co-rich region as well as Co-poor region. In case of Cu and Nd, however, the eutectic decomposition occurs at $\sim 500^\circ\text{C}$, thus there is no chance to form Cu-rich phase from eutectic reaction during 2nd PSA. Also, Cu has no solubility to the main magnetic phase at 2nd PSA temperature and Cu can move towards the Co-poor region resulting in the formation of Cu-rich phase [13].

Fig. 4 shows TEM bright field and SADP images of Nd-rich TJP in the DyF_3 dipped magnet (a,c) and DyCo source coated magnet (b,d). The crystal structure analysis revealed that the DyCo coated magnet was c- Nd_2O_3 but the Dy Compound coated magnet was h- Nd_2O_3 phase. c- Nd_2O_3 phase was stabilized when Co, Cu segregation was more than 30 at. %, hence increasing

the coercivity by reducing the interfacial lattice mismatch [13]. The formation of stable c- Nd_2O_3 phase in TJP, although Co segregated in the TJP, seemed to be the reason of the coercivity enhancement in GBDP.

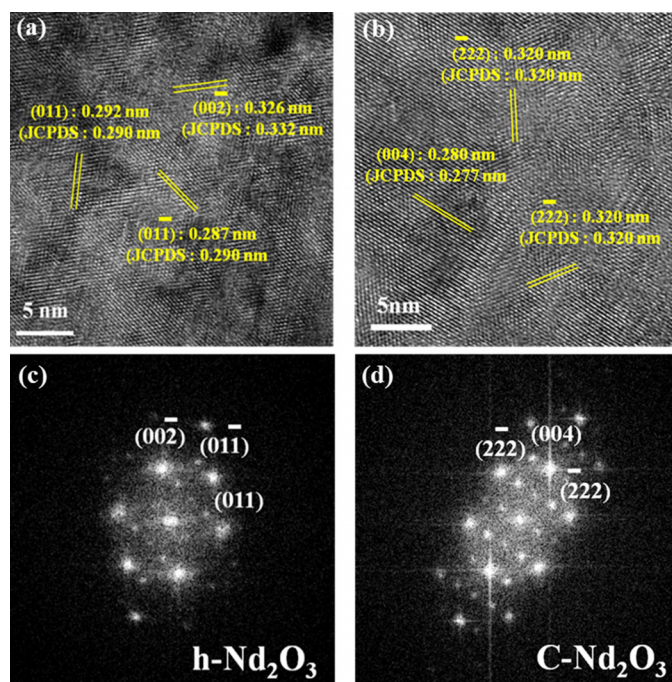


Fig. 4. HR-TEM micrograph and corresponding SADP images of (a), (c) DyF_3 dipped magnet and (b), (d) DyCo dipped magnets

4. Conclusions

The magnetic and microstructure characteristics of the NdFeB sintered magnet dipped in DyCo, Cu + DyCo and Al + DyCo solutions were investigated. The coercivity of the Al + DyCo dipped magnet was higher than those of the Cu + DyCo

dipped magnet and the magnet dipped in DyCo only, even though they all formed core-shell type structures. Cu and Al acted as the carriers of Dy atoms so that relatively large number of Dy atoms diffused into the magnet's interior from the Dy-source coated surface. The Cu/Al-rich grain boundary phase might have enhanced the diffusivity of Dy atoms. Large number of Dy atoms reached into the magnet and mostly segregated at the interface of Nd₂Fe₁₄B and grain boundary phases covering Nd₂Fe₁₄B grains to form core-shell type structures. The formation of highly anisotropic (Nd, Dy)₂Fe₁₄B phase layer due to Dy diffusion is responsible to screen the reverse domain movement by forming shells in the core-shell type structures. This was the main cause of the enhanced coercivity of diffusion treated NdFeB magnets.

Acknowledgments

This work is supported by the Strategic Core Material Technology Development Program (No10043780) funded by the ministry of Trade, Industry and Energy (Korea)

REFERENCES

- [1] K. Hirota, H. Nakamura, T. Minowa, M. Hoshima, IEEE Trans. Magn. **42**, 2909-2911 (2006).
- [2] H. Sepehri-Amin, T. Ohkubo, K. Hono, J. Appl. Phys. **107**, 09A745 (2010).
- [3] K.H.J. Buschow, J. Mater. Sci. Res. **1**, 1-64 (1986).
- [4] J. Fidler, J. Bernardi, J. Appl. Phys. **70**, 6456-6458 (1991).
- [5] D.S. Li, S. Suzuki, T. Kawasaki, K. Machida, Jpn. J. Appl. Phys. **47**, 7876-7878 (2008).
- [6] K. Hirota, H. Nakamura, T. Minowa, M. Honshima, IEEE Trans. Magn. **41**, 2909-2911 (2006).
- [7] D.S. Li, M. Nishimoto, S. Suzuki, K. Nishiyama, M. Itoh, K. Machida, 2009 IOP Conf. Ser.: Mater. Sci. Eng. **1**, 012020 (2009).
- [8] M. Komuro, Y. Satsu, H. Suzuki, IEEE Trans. Magn. **46**, 3831-3833 (2010).
- [9] B.E. Davies, R.S. Mottram, I.R. Harris, J. Mater. Chem. Phys. **64**, 272-281 (2001).
- [10] A. Kowalczyk, A. Wrzeciono, J. Magn. Magn. Mater. **74**, 260 (1988).
- [11] W.F. Li, T. Ohkubo, T. Akiya, H. Kato, K. Hono, J. Mater. Res. **24**, 413 (2009).
- [12] S. Hirohara, Y. Matsuura, H. Yamamoto, S. Fujimura, M. Sagawa, H. Yamauchi, J. Appl. Phys. **59**, 873-879 (1986).
- [13] T.N. Rezhukhina, T.F. Sisoeva, J. Chem. Thermodynamics. **11**, 1095-1099 (1979).
- [14] J.A. Kerr, CRC Handbook of Chemistry and Physics 1999-2000 : A Ready-Reference Book of Chemical and Physical Data **81** st es., USA (2000).
- [15] H. Nakamura, K. Hirota, M. Shimao, T. Minowa, M. Honshima, IEEE. Tran. Magn. **41**, 3844-3946 (2005).
- [16] D.W. Park, T.H. Kim, S.R. Lee, D.H. Kim, T.S. Jang, J. Appl. Phys., **107**, 09A737-1-09A737-3 (2010).